Improved regenerative myogenesis and muscular dystrophy in mice lacking *Mkp5*

Hao Shi,[1] Mayank Verma,[1] Lei Zhang,[1] Chen Dong,[2] Richard A. Flavell,[3] and Anton M. Bennett[1,4]

[1]Department of Pharmacology, Yale University School of Medicine, New Haven, Connecticut, USA. [2]Department of Immunology, The University of Texas MD Anderson Cancer Center, Houston, Texas, USA. [3]Department of Immunobiology and Howard Hughes Medical Institute, and [4]Program in Integrative Cell Signaling and Neurobiology of Metabolism, Yale University School of Medicine, New Haven, Connecticut, USA.

Duchenne muscular dystrophy (DMD) is a degenerative skeletal muscle disease caused by mutations in dystrophin. The degree of functional deterioration in muscle stem cells determines the severity of DMD. The mitogen-activated protein kinases (MAPKs), which are inactivated by MAPK phosphatases (MKPs), represent a central signaling node in the regulation of muscle stem cell function. Here we show that the dual-specificity protein phosphatase DUSP10/MKP-5 negatively regulates muscle stem cell function in mice. MKP-5 controlled JNK to coordinate muscle stem cell proliferation and p38 MAPK to control differentiation. Genetic loss of *Mkp5* in mice improved regenerative myogenesis and dystrophin-deficient *mdx* mice lacking *Mkp5* exhibited an attenuated dystrophic muscle phenotype. Hence, enhanced promyogenic MAPK activity preserved muscle stem cell function even in the absence of dystrophin and ultimately curtailed the pathogenesis associated with DMD. These results identify MKP-5 as an essential negative regulator of the promyogenic actions of the MAPKs and suggest that MKP-5 may serve as a target to promote muscle stem cell function in the treatment of degenerative skeletal muscle diseases.

Introduction

Muscle precursor cells, known as satellite cells (SCs), govern the maintenance and repair of adult skeletal muscle (1–5). Located between the basal lamina and sarcolemma, SCs are quiescent in nature and respond to regenerative cues such as physical damage or exercise by undergoing cycles of proliferation before terminally differentiating into multinucleated myofibers (1, 2, 6, 7). SCs are the primary cell type through which adult regenerative myogenesis is mediated, and loss of SC function contributes to degenerative skeletal muscle diseases (5–12). Duchenne muscular dystrophy (DMD) is a devastating X-linked recessive genetic disorder affecting approximately 1 in 3,500 male births worldwide (13). DMD is caused by mutations in the dystrophin gene, which result in a lack of dystrophin protein expression (13, 14). In DMD, skeletal muscle regeneration is severely impaired due to the depletion of SCs as a result of a futile cycle of degeneration and regeneration. Ultimately, DMD patients lose muscle strength and mobility, and the disease often results in death. There is neither a cure, nor an effective treatment for DMD (9, 15). Because the progression of DMD is associated with deteriorating SC functionality (9), understanding the mechanisms of SC control will provide insight into new therapeutic strategies for the treatment of DMD.

An important aspect of SC biology is the ability of SCs to proliferate in response to injury. Myoblasts from DMD patients exhibit impaired proliferation (16). More recently, mice lacking the expression of dystrophin (*mdx*), which represents a mouse model of DMD, exhibit an exacerbated progression of muscle degeneration when the RNA component of telomerase is deleted (17). SCs derived from *mdx* mice with the defective telomerase have an impaired regenerative capacity that is attributed, in part, to a reduced capacity of SCs from these mice to proliferate (17). Hence, the replicative capacity of SCs plays a critical role in the maintenance and repair of skeletal muscle.

The ability of SCs to proliferate and differentiate in order to effectively repair damaged skeletal muscle requires both coordinated activation and inactivation of signaling pathways. Although there has been much emphasis placed on the signals that initiate SC proliferation and differentiation, there is still relatively little known about the signaling pathways that promote the cessation of regenerative myogenesis. One of the more prominent signaling pathways involved in the initiation of regenerative myogenesis is the mitogen-activated protein kinase (MAPK) pathway. Of the 3 major MAPK family members, the p38 MAPK subfamily, in particular p38 α/β MAPKs, referred to herein as p38 MAPK, have figured most prominently in promyogenic signaling to promote SC function (18–24). Although p38 MAPK is considered unequivocally to be a promyogenic MAPK, the role of other MAPK family members, such as the extracellular signal-regulated kinases 1 and 2 (ERK1/2) and the c-Jun NH_2 terminus kinases (JNKs), has been less clear. ERK1/2 has been shown to exhibit both positive and negative regulatory roles in myogenesis (25–29), and JNK appears in some cases to be either dispensable or negative in myogenesis (30–32). Therefore, the role of ERK1/2 and JNK in regenerative myogenesis has yet to be conclusively resolved.

Despite the established contribution of the MAPKs, such as p38 MAPK, in SC promyogenic signaling and regenerative myogenesis, it is unclear how MAPKs are temporally inactivated in order to terminate myogenesis. One mechanism likely involves the coordinated inactivation of the promyogenic MAPKs by the MAPK phosphatases (MKPs). The MKPs constitute a family of 10 dual-specificity phosphatases (DUSPs) that exhibit the capacity to specifically dephosphorylate MAPKs on the regulatory threonine and tyrosine residues (33–36). However, the identity of the physiologically relevant MKP that inactivates the promyogenic MAPKs in SCs, and then curtails regenerative myogenesis, has yet to be determined. Previous work has suggested a role for MKP-1 in regenerative myogenesis (20, 37), muscle growth (38–42), and skeletal muscle regeneration (43). MKP-1–deficient SCs have impaired

Conflict of interest: The authors have declared that no conflict of interest exists.
Citation for this article: *J Clin Invest.* 2013;123(5):2064–2077. doi:10.1172/JCI64375.

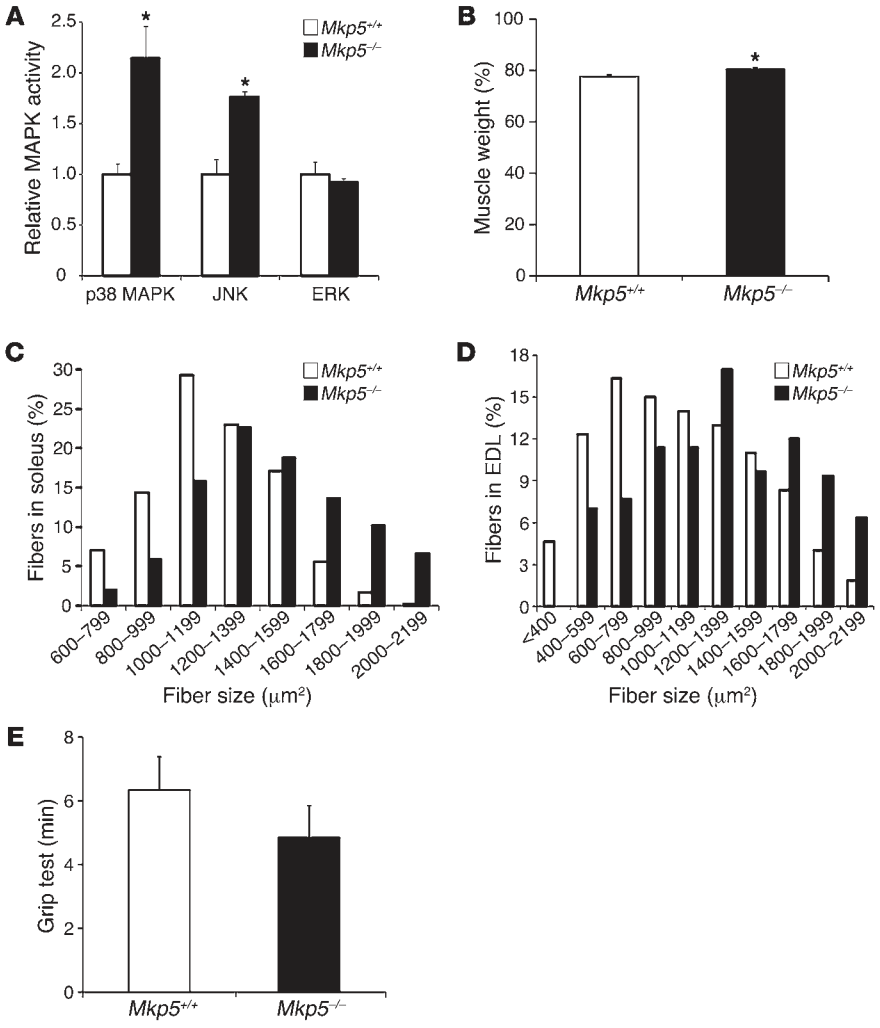

Figure 1
MKP-5 deficiency enhances skeletal muscle MAPK activity, muscle mass, and fiber size. (**A**) Fold change of MAPK activities in TA muscle measured by immune complex kinase assays (n = 4 littermates per genotype). (**B**) Whole-body muscle composition in 8-week-old male mice were analyzed using a Bruker's minispec Whole Body Composition Analyzer (n = 7 per genotype). (**C** and **D**) Histograms of muscle fiber size in soleus (**C**) and EDL (**D**) muscles. Five hundred fibers from 4 littermates were counted per genotype. (**E**) Grip test. Mice were assessed for limb strength (n = 7 per genotype). Results are the mean ± SEM. *P < 0.05 compared with *Mkp5*$^{+/+}$ mice. (**A**–**E**) Represent data collected from 8-week-old male mice.

proliferation and differentiate precociously (43). Moreover, when crossed on to the *mdx* background, MKP-1–deficient mice exhibit an exacerbated muscular dystrophinopathy compared with *mdx* mice (43). These findings suggest that MKP-1 promotes, rather than attenuates, SC function and regenerative myogenesis. In light of these results, it remains unclear how p38 MAPK and other MAPKs that are involved in regenerative myogenesis are maintained in a low state of activity, as would be the prediction in quiescent SCs. Moreover, how these MAPKs are coordinately inactivated once SC proliferation and differentiation have been completed remains to be determined.

In this study, we investigated the role of the dual-specificity phosphatase, DUSP10/MKP-5, in SC function and regenerative myogenesis. MKP-5 is a cytosolic and nuclear MKP (34) that has been implicated in innate immune responses (44) and vascular inflammation (45) in mice. Here, we show that MKP-5 negatively regulates SC proliferation and differentiation by selectively dephosphorylating JNK and p38 MAPK, but not ERK1/2, in a temporal manner during regenerative myogenesis. Consistent with this, mice lacking MKP-5 expression exhibit improved regenerative myogenesis. Remarkably, *mdx* mice lacking MKP-5 are protected from progressive muscular dystrophinopathy and demonstrate preserved skeletal muscle function. Collectively, these findings define MKP-5 as a critical negative regulator of the promyogenic MAPKs in SCs. These data suggest that MKP-5 may serve as a potential therapeutic target for the treatment of degenerative muscle diseases.

Results

Increased MAPK activity, enhanced skeletal muscle mass, and regenerative myogenesis in MKP-5–deficient mice. MKP-5 is highly enriched in skeletal muscle (46, 47), suggesting that it may play an important role in this tissue. In order to determine whether MKP-5 plays a role in skeletal muscle function, we examined the skeletal muscle phenotype in mice lacking MKP-5 (*Mkp5*$^{-/-}$) expression (44). We found that uninjured *Mkp5*$^{-/-}$ mice exhibited increased skeletal muscle JNK and p38 MAPK, but not ERK1/2, activity compared with *Mkp5*$^{+/+}$ mice (Figure 1A). *Mkp5*$^{-/-}$ mice exhibited increased skeletal muscle mass and skeletal muscle fiber size compared with *Mkp5*$^{+/+}$ mice (Figure 1, B–D, and Supplemental Figure 1, A–D; supplemental material available online with this article; doi:10.1172/JCI64375DS1). Although *Mkp5*$^{-/-}$ mice had increased skeletal muscle mass, this did not result in an appreciable difference in muscle strength since grip strength performance was comparable between *Mkp5*$^{-/-}$ and *Mkp5*$^{+/+}$ mice (Figure 1E). These results demonstrate that MKP-5 plays a role in the negative regulation of skeletal mus-

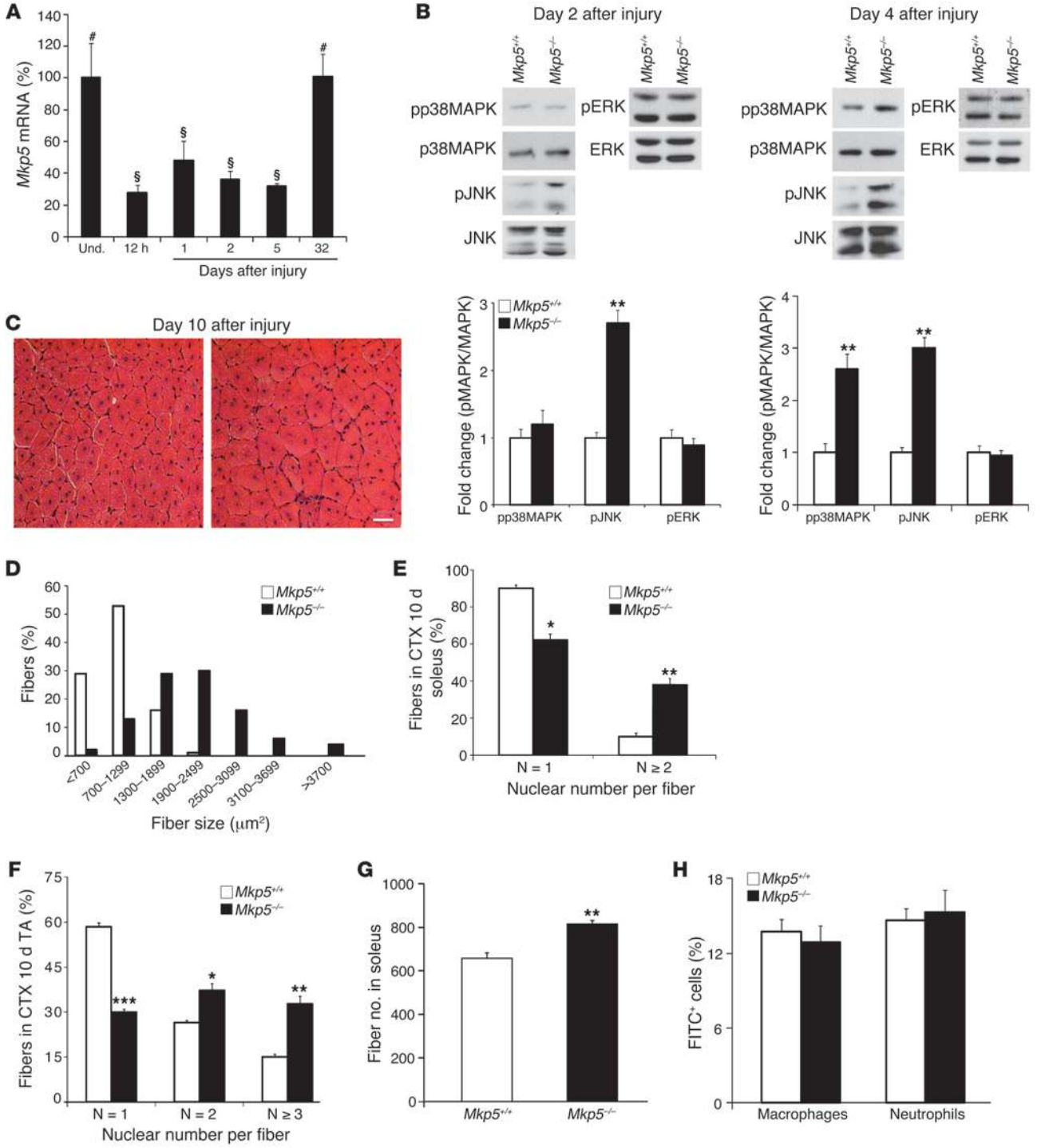

Figure 2

MKP-5 negatively regulates regenerative myogenesis. (**A**) TA muscles from wild-type C57BL/6 mice were damaged by CTX injection, and MKP-5 transcripts were measured by quantitative PCR and expressed as a percentage of control (n = 4–5 per time point). Symbols that differ (# and §) signify statistical significance between time points; $P < 0.05$. (**B**) Fold change of phosphorylated MAPKs at days 2 (left panel) and 4 (right panel) after CTX damage (n = 9 per genotype). (**C**) Ten days after CTX-induced damage, TA muscles were prepared for H&E staining. Scale bar: 50 μm. (**D**) Histogram showing nascent myofiber size 10 days after injury in TA muscle (n = 5 per genotype). (**E** and **F**) Number of myonuclei (N) per nascent myofiber was counted 10 days after soleus (**E**) and TA (**F**) muscle injury (n = 5 per genotype). (**G**) Ten days after CTX injury, the total number of muscle fibers in soleus muscle was counted (n = 6 per genotype). (**H**) Forty-two hours after CTX-induced muscle damage, cells from TA muscle were isolated and FACS analyzed for macrophages and neutrophils (n = 6 per genotype). Results are the mean ± SEM. *$P < 0.05$; **$P < 0.01$; and ***$P < 0.001$ compared with wild-type mice. (**A**–**H**) All mice were 8-week-old males. Und., undamaged.

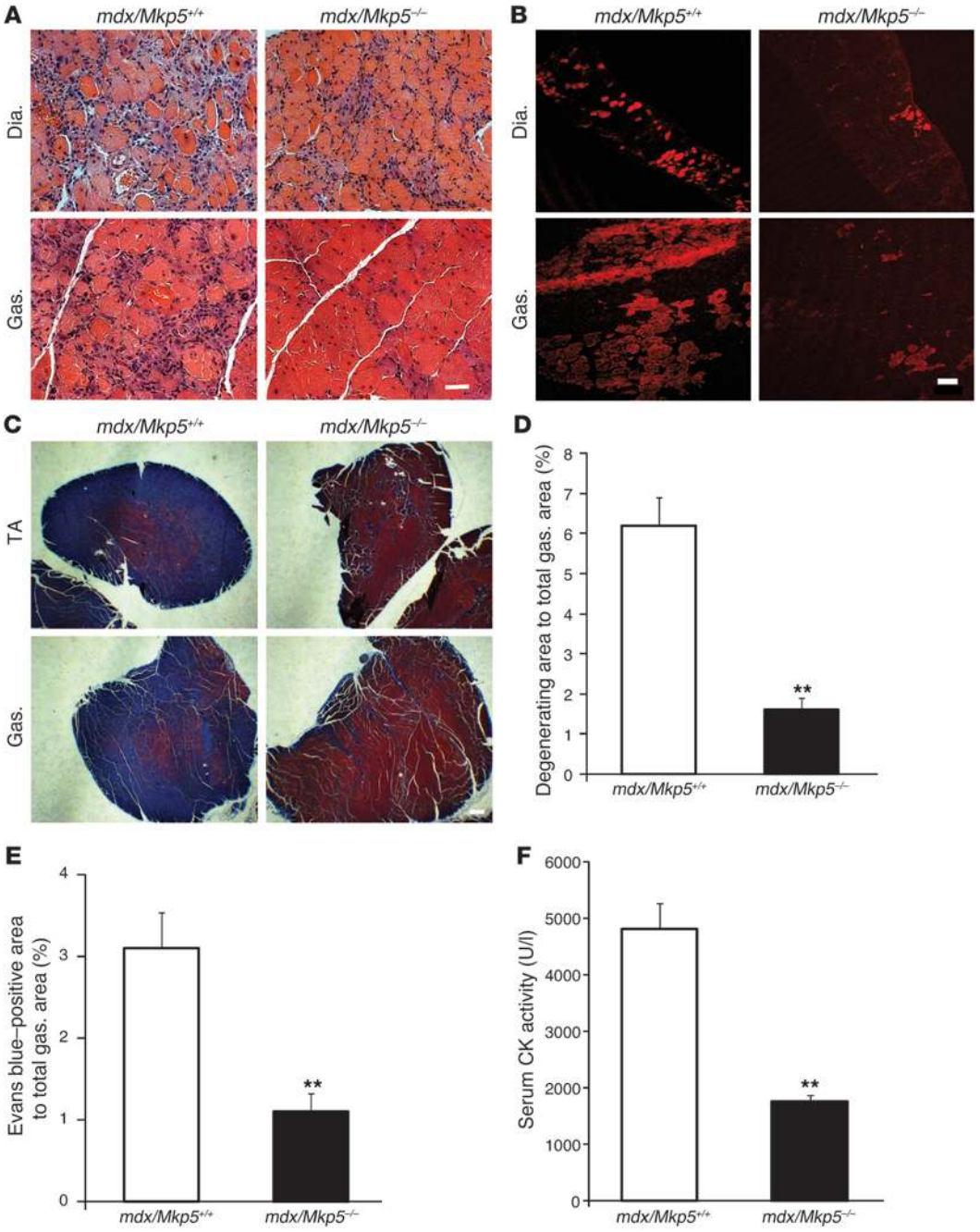

Figure 3
MKP-5 deficiency in *mdx* mice leads to ameliorated myopathy. (**A**) H&E staining of the diaphragm (Dia.) and gastrocnemius (Gas.) muscles. Scale bar: 50 μm. (**B**) Evans blue dye uptake. Scale bar: 100 μm. (**C**) Masson's trichrome staining. Scale bar: 300 μm. (**D**) Degenerating area percentage (>10 degenerating myofibers) of total gastrocnemius muscle sections. (**E**) Evans blue dye area percentage of the gastrocnemius section. (**A**–**E**) $n = 6$ per genotype; mice were 3-month-old males. (**F**) Serum creatine kinase (CK) activity ($n = 6$ per genotype; 4-month-old male mice). Results are the mean ± SEM. $^{**}P < 0.01$ compared with *mdx*/*Mkp5*$^{+/+}$ mice.

cle p38 MAPK and JNK activity, but not ERK1/2 activity, in the suppression of skeletal muscle growth.

To investigate the role of MKP-5 in adult skeletal muscle regeneration, we induced skeletal muscle damage by cardiotoxin (CTX) injection. MKP-5 expression was significantly reduced following muscle damage and returned to levels equivalent to those of undamaged muscle approximately 1 month after injury (Figure 2A). During skeletal muscle regeneration, MAPK hyperactivation in skeletal muscles from *Mkp5*$^{-/-}$ mice was initially selective for JNK, which had increased activity 2 days after damage, and by 4 days after injury, activity for both JNK and p38 MAPK was increased (Figure 2B). These results suggest that MKP-5 is essential for the negative regulation of JNK both early and late after injury. In contrast, p38 MAPK appears to be the predominant target of MKP-5 later on during regenerative myogenesis. No differences in ERK1/2 phosphorylation were observed at either 2 or 4 days after injury between *Mkp5*$^{+/+}$ and *Mkp5*$^{-/-}$ mice (Figure 2B). Newborn myofibers at 10 days after injury in *Mkp5*$^{-/-}$ mice were larger in diameter (Figure 2, C and D) and contained more nuclei per myofiber compared with *Mkp5*$^{+/+}$ mice at the same stage after injury (Figure 2, E and F). The enhanced regenerative myogenesis observed in the skeletal muscle of *Mkp5*$^{-/-}$ mice was also accompanied by a significant increase in the total number of myofibers (Figure 2G). We interpret these results to suggest that MKP-5 neg-

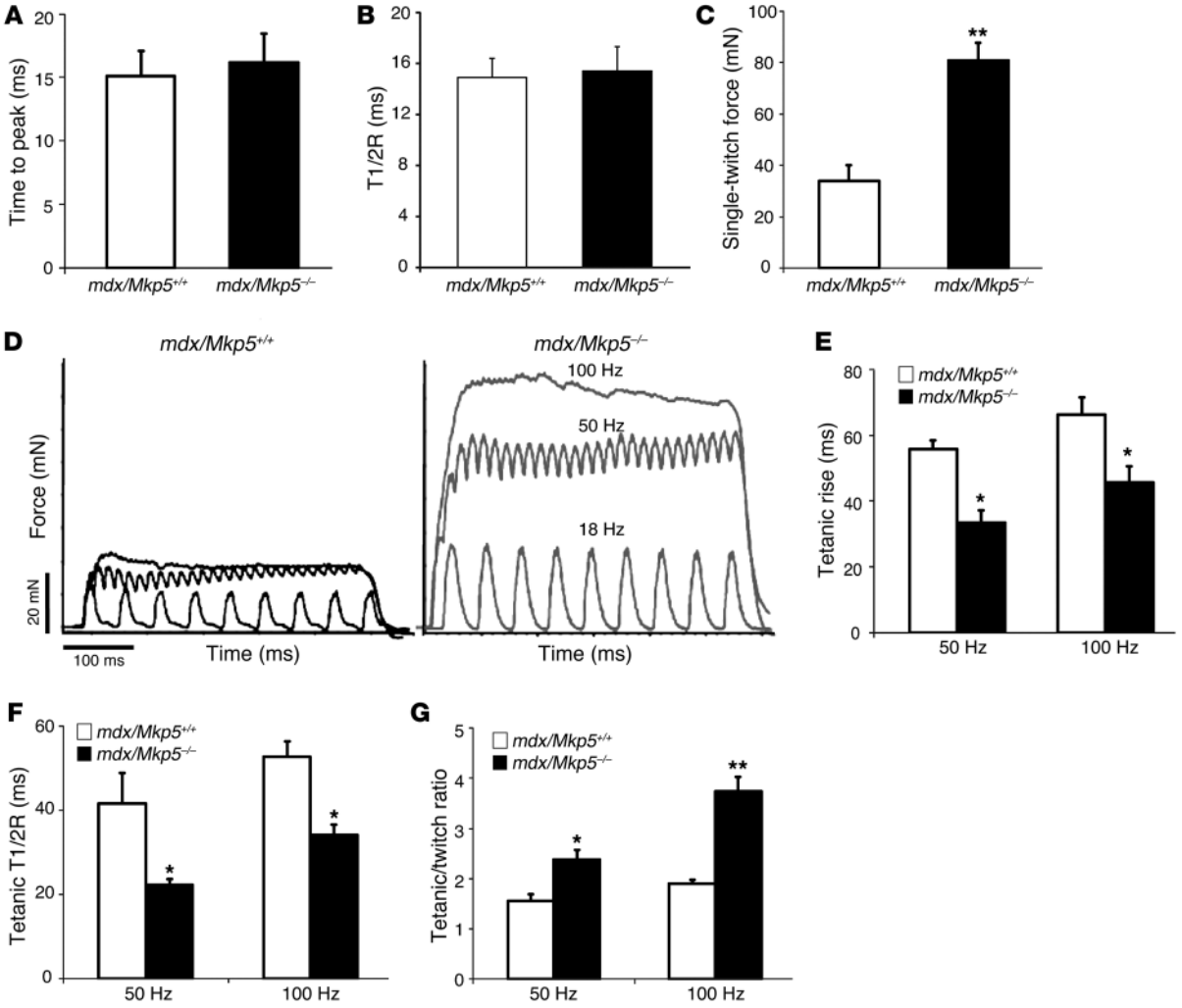

Figure 4
EDL muscle contractile properties of MKP-5–deficient *mdx* mice. (**A**–**C**) Single-twitch contraction. (**A**) Time to peak, (**B**) time to half-relaxation (T1/2R), and (**C**) single-twitch force were recorded after a single stimulation. (**D**) EDL muscle contraction electrographs were generated by inducing EDL muscle with 500-millisecond train stimulation at 18, 50, and 100 Hz. (**E**–**G**) Tetanic force was induced in EDL muscle with 100-Hz stimulation. (**E**) Tetanic rise time, (**F**) tetanic time to half-relaxation (T1/2R), and (**G**) tetanic/twitch force ratio. **P* < 0.05 and ***P* < 0.01 compared with *mdx*/*Mkp5*$^{+/+}$ mice. Data represent the mean ± SEM (*n* = 6 per genotype; 3-month-old male mice).

atively regulates JNK and p38 MAPK in a temporal manner during regenerative myogenesis and that loss of MKP-5 results in an enhanced regenerative response following acute muscle injury.

MKP-5 has been reported to participate in the inflammatory response (44, 45), and our previous work suggested that MKPs, such as MKP-1, regulate inflammation during muscle repair (43). We tested whether MKP-5 behaved similarly. Neither macrophage nor neutrophil infiltration was found to be significantly different in the damaged areas of skeletal muscle between *Mkp5*$^{+/+}$ and *Mkp5*$^{-/-}$ mice (Figure 2H). Cytokine levels were not profoundly different, although IL-6 and IFN-γ were increased in the damaged skeletal muscles of *Mkp5*$^{-/-}$ mice (Supplemental Table 1). Therefore, in skeletal muscle, MKP-5 does not appear to profoundly influence the infiltration of hematopoietic cells into the damaged area.

Protection from dystrophic muscle disease in MKP-5–deficient mdx mice. Skeletal muscle in the *mdx* mouse displays a dystrophic muscle phenotype, especially in the diaphragm (48). To investigate whether MKP-5 is also involved in exerting a negative effect on adult regenerative myogenesis in DMD, we intercrossed *Mkp5*$^{-/-}$ mice into the *mdx* background in order to generate *mdx/Mkp5*$^{+/+}$ and *mdx/Mkp5*$^{-/-}$ mice. As anticipated, *mdx/Mkp5*$^{-/-}$ mice exhibited increased p38 MAPK and JNK phosphorylation, but not ERK1/2 phosphorylation, compared with *mdx/Mkp5*$^{+/+}$ mice (Supplemental Figure 2, A and B). These results demonstrate that loss of dystrophin does not interfere with the ability of MKP-5 to negatively regulate p38 MAPK and JNK. Improved skeletal muscle morphology and significantly reduced levels of degenerating muscle fibers were observed in the diaphragm and gastrocnemius of *mdx/Mkp5*$^{-/-}$ mice (Figure 3A). Evans blue dye uptake, an indicator of the loss of skeletal muscle fiber membrane integrity, was significantly reduced in *mdx/Mkp5*$^{-/-}$ mice compared with *mdx/Mkp5*$^{+/+}$ mice (Figure 3B). The onset of fibrosis, a hallmark of progression

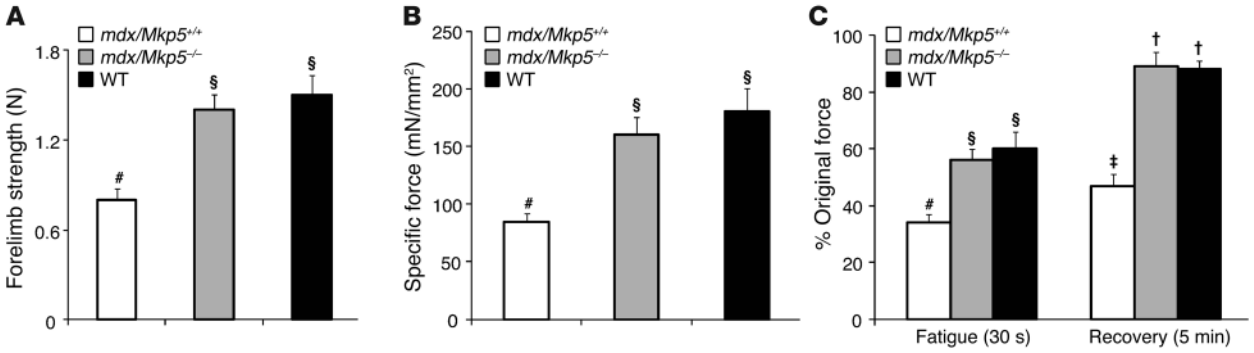

Figure 5

MKP-5 deficiency in *mdx* mice leads to restored muscle function. (**A**) Forelimb muscle strength measurement using a grip strength meter (Columbus Instruments). (**B**) EDL muscle–specific force. Tetanic contraction produced by stimulation at 100 Hz. (**C**) EDL muscle fatigue and relaxation. Muscles were subjected to a fatigue protocol consisting of a 1-second, 100-Hz tetanus every 2 seconds for a total of 30 seconds. Recovered force was measured by stimulating the EDLs for 250 milliseconds with 100-Hz pulses. Symbols that differ (#, §, ‡, or †) signify statistical significance at $P < 0.05$. Results are the mean ± SEM ($n = 6$ per genotype; 3-month-old male mice).

of the dystrophic phenotype, was markedly reduced in the skeletal muscles of *mdx/Mkp5*$^{-/-}$ mice compared with those of *mdx/Mkp5*$^{+/+}$ mice (Figure 3C). To quantify the extent of the damage, we measured the areas that contained more than 10 degenerating myofibers and expressed this as a percentage of the total muscle cross-sectional area of the gastrocnemius muscle (49). We found that the damaged areas were greatly reduced in *mdx/Mkp5*$^{-/-}$ muscle (Figure 3D). We also quantified damaged fibers by determining the areas of fibers that became permeable to Evans blue dye. We found that *mdx/Mkp5*$^{-/-}$ muscles had a significantly reduced area of fibers that were Evans blue–positive (Figure 3E). The extent to which a lack of MKP-5 ameliorated the progression of the dystrophic phenotype was further supported biochemically through measures of serum creatine kinase (CK) activity, which was significantly decreased in *mdx/Mkp5*$^{-/-}$ mice (Figure 3F). Together, these findings demonstrate that a lack of MKP-5 ameliorates muscular dystrophinopathy in *mdx* mice.

To further examine whether the improved myopathy in MKP-5–deficient *mdx* mice reflects the recovery of skeletal muscle function, we tested the muscle contractile properties in *mdx/Mkp5*$^{+/+}$ and *mdx/Mkp5*$^{-/-}$ mice. No basal differences in gross muscle strength were observed between *Mkp5*$^{+/+}$ and *Mkp5*$^{-/-}$ mice (Figure 1E). Hence, *Mkp5*$^{-/-}$ mice were not developmentally distinct in broad muscle contractile properties compared with *Mkp5*$^{+/+}$ mice. On the *mdx* background, MKP-5 deficiency revealed no detectable change in the velocities of contraction or relaxation in a single stimulation compared with wild-type mice (Figure 4, A and B). However, several parameters of muscle function were significantly improved in *mdx/Mkp5*$^{-/-}$ mice compared with *mdx/Mkp5*$^{+/+}$ mice (Figure 4, C–G). Extensor digitorum longus (EDL) muscle single-twitch force (Figure 4C) and tetanic force (Figure 4D) were significantly increased in the muscles of *mdx/Mkp5*$^{-/-}$ mice compared with those of *mdx/Mkp5*$^{+/+}$ mice. The time to rise to tetanus (Figure 4E) and the time to release after tetanus (Figure 4F) were markedly reduced, indicating that the responsiveness of *mdx/Mkp5*$^{-/-}$ mouse EDL muscles to stimuli is significantly improved. The tetanic/twitch force ratio, an indicator of muscle force buildup, increased significantly in *mdx/Mkp5*$^{-/-}$ EDL muscle compared with *mdx/Mkp5*$^{+/+}$ EDL muscle (Figure 4G). Taken together, these parameters indicate that MKP-5 deficiency in the *mdx* model of myopathy impairs the deterioration of muscle contractile function, an observation that is consistent with the improved skeletal muscle morphology in *mdx/Mkp5*$^{-/-}$ mice (Figure 3).

To further define the extent to which a lack of MKP-5 maintains skeletal muscle function, we compared *mdx/Mkp5*$^{+/+}$ and *mdx/Mkp5*$^{-/-}$ mice with wild-type C57BL/10 mice. Consistent with the reduced severity of the dystrophic phenotype, *mdx/Mkp5*$^{-/-}$ mice exhibited equivalent levels of skeletal muscle function, as determined by forelimb strength, when compared with wild-type (C57BL/10) mice (Figure 5A). Furthermore, the specific force of EDL muscle was preserved to levels equivalent to those of the wild-type (C57BL/10) mice (Figure 5B). Additionally, *mdx/Mkp5*$^{-/-}$ mice showed resistance to repeated contraction-induced fatigue at levels equivalent to those of wild-type (C57BL/10) mice, whereas EDL muscles from *mdx/Mkp5*$^{+/+}$ mice were significantly impaired in their ability to recover (Figure 5C). These findings demonstrate that loss of MKP-5 ameliorates the progression of the dystrophic phenotype in *mdx* mice. Since SC dysfunction likely underlies the cellular basis of the dystrophic phenotype, these results strongly suggest that SCs represent a major site of MKP-5 action.

MKP-5 negatively regulates SC proliferation and differentiation. In order to elucidate the cause of the enhanced skeletal muscle regenerative capacity in *Mkp5*$^{-/-}$, mice we measured SC expansion in response to injury by enumerating PAX7^{+} SCs in muscle cross sections 10 days after injury (50). In response to injury, the SC population expanded by 88.7% in *Mkp5*$^{-/-}$ mice compared with 36.9% in *Mkp5*$^{+/+}$ mice (Supplemental Figure 3, A–C). These results suggest that MKP-5–deficient SCs are hyperproliferative. Consistent with this, SC-derived myoblasts from *Mkp5*$^{-/-}$ mice exhibited increased proliferative capacity as determined using either a clonal assay in single myofiber explants (Figure 6A) or in FACS-sorted SC cultures (Figure 6B). In order to rule out the possibility that SC-derived myoblasts were hyperproliferative due to a developmentally acquired property of *Mkp5*$^{-/-}$ mice, we isolated SC-derived myoblasts from adult wild-type mice. These SC-derived myoblasts were then subjected to MKP-5 knockdown using siRNA (Figure 6C). Under these conditions, *Mkp5* expression was reduced by greater than 80% in nontargeted siRNA–treated SC-derived myoblasts (Supplemental Figure 4, A and B). MKP-5 siRNA–treated SC-derived myoblasts had increased

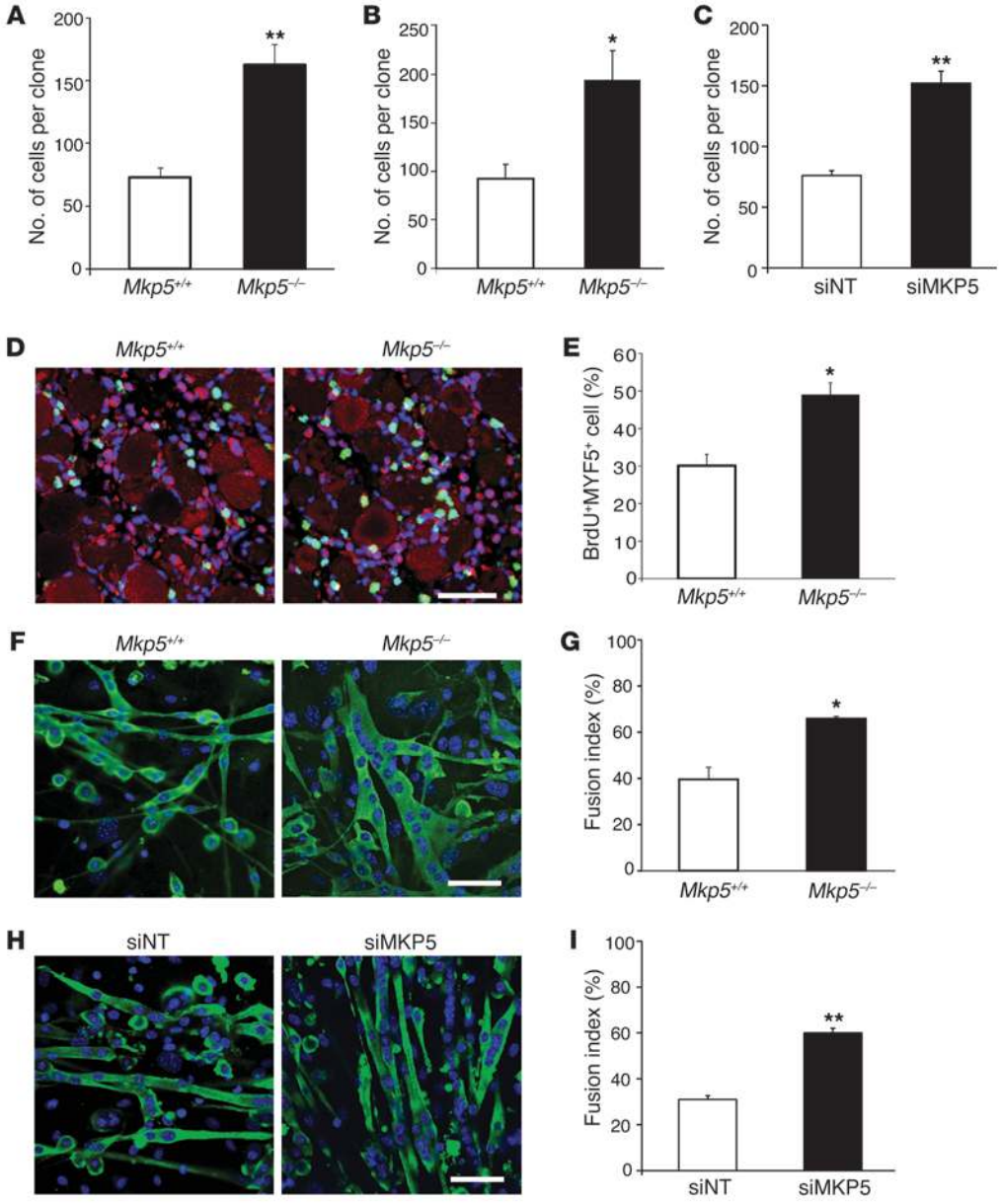

Figure 6

MKP-5 represses the proliferative and differentiative capacity of SCs. (**A**) Clonal assay from single myofiber explants cultured in growth medium (GM) for 6 days (n = 3 independent preparations). (**B**) Clonal assay from FACS-sorted SCs were cultured in GM for 7 days (n = 3 independent preparations). (**C**) Clonal assay from nontargeted and MKP-5 siRNA knockdown SCs isolated from C57BL/6J muscles. Cells were cultured in GM for 7 days (n = 3 independent preparations). (**D**) Gastrocnemius muscles were CTX injured for 24 hours and injected with BrdU; 18 hours later, cells were analyzed for BrdU and MYF5 expression (n = 5 per genotype). Photomicrographs show representative images of stained sections: MYF5 (pink); nuclei (blue); BrdU (green); nonspecific staining (red). Scale bar: 50 μm. Percentage of BrdU$^+$/MYF5$^+$ cells are quantified in **E**. (**F**) SCs were seeded at equal cell numbers to reach 90% confluence the next day, then the growth medium was switched to differentiation medium for 3 days. Cells were stained for myosin heavy chain (green) and nuclei (blue). Scale bar: 50 μm. (**G**) Fusion index was calculated as a percentage of nuclei in myotubes with greater than or equal to 2 nuclei divided by the total number of nuclei (n = 3 independent preparations). (**H**) SCs differentiated for 3 days after MKP-5 knockdown were stained for myosin heavy chain (green) and nuclei (blue). Scale bar: 50 μm. (**I**) Fusion index calculated as in **G** (n = 3 independent preparations). (**A**–**I**) All mice were 8-week-old males. For each independent preparation, 2 mice per genotype were used. Data represent the mean ± SEM. *P < 0.05 and **P < 0.01 compared with the *Mkp5*$^{+/+}$ or nontargeted siRNA–treated group.

proliferation levels compared with nontargeted siRNA–treated myoblasts (Figure 6C). To directly assess SC proliferation in vivo, skeletal muscle was damaged and BrdU was injected 24 hours after injury. The percentage of SCs (MYF5$^+$) that were BrdU$^+$ was significantly increased in *Mkp5*$^{-/-}$ mice compared with *Mkp5*$^{+/+}$ mice (Figure 6, D and E). These results demonstrate that MKP-5 exerts autonomous negative regulation of postdevelopmental SC proliferation in adult mice.

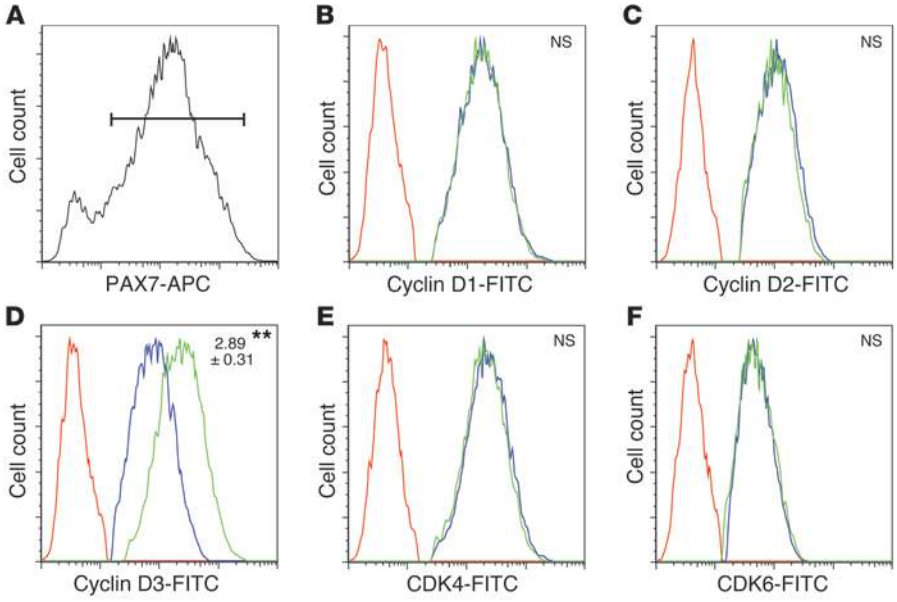

Figure 7
MKP-5 deficiency increases the expression of cyclin D3 in SCs. Eight-week-old male mouse hind limb muscles were damaged by CTX, and 48 hours later muscles were dissected and digested to isolate cells for flow cytometry. Gated (PAX7$^+$) cells (**A**) were analyzed for cyclin D1 (**B**), cyclin D2 (**C**), cyclin D3 (**D**), CDK4 (**E**), and CDK6 (**F**). No stain control (red); *Mkp5*$^{+/+}$ (blue); *Mkp5*$^{-/-}$ (green). Data represent 3 independent experiments with 2 mice from each genotype in each independent experiment. Protein content was evaluated by measuring the median fluorescence intensity and expressed as fold change relative to *Mkp5*$^{+/+}$. $^{**}P < 0.01$ compared with *Mkp5*$^{+/+}$ mice. NS, not statistically significant.

Next, we evaluated the effects of MKP-5 on SC differentiation. SC-derived myoblasts from *Mkp5*$^{-/-}$ mice differentiated more robustly with a significantly increased level of myoblasts fusing into multinucleated myotubes compared with that in *Mkp5*$^{+/+}$ SCs (Figure 6, F and G). Similarly, MKP-5 siRNA–treated SC-derived myoblasts from wild-type mice also had enhanced capacity to undergo fusion into multinucleated myotubes (Figure 6, H and I). These results demonstrate that MKP-5 negatively regulates both SC proliferation and differentiation, suggesting that loss of MKP-5 in SCs gives rise to enhanced SC function, which is likely causal to the improved regenerative capacity and ameliorative dystrophic response observed in mice lacking MKP-5.

MKP-5 negatively regulates cyclin D3 expression in regenerating skeletal muscle. To examine the molecular mechanisms of MKP-5 regulation of regenerative myogenesis in mice, we assessed the expression of cell-cycle regulatory proteins in regenerating skeletal muscles from *Mkp5*$^{+/+}$ and *Mkp5*$^{-/-}$ mice. Although SCs represent between 1% and 2% of total skeletal muscle mass, the population of SCs dramatically expands during regeneration. We hypothesized that changes in the expression of cell-cycle regulatory proteins in skeletal muscle will likely reflect similar changes of these proteins in the population of proliferating SCs early on during regenerative myogenesis. We found that 2 days following muscle regeneration, cyclin D3 expression, but not D1 or D2 expression, was increased in *Mkp5*$^{-/-}$ skeletal muscle (Supplemental Figures 5 and 6). Consistent with the observation of enhanced skeletal muscle regeneration, it has been reported that cyclin D3 promotes myoblast proliferation, cell-cycle exit, and differentiation (51, 52). No appreciable differences in CDK4, CDK6, or p15^{INK4b} levels were observed (Supplemental Figures 5 and 6). In line with the increased cyclin D3 levels, Rb was phosphorylated to a greater extent in regenerating skeletal muscle from *Mkp5*$^{-/-}$ mice compared with *Mkp5*$^{+/+}$ mice (Supplemental Figures 5 and 6). In agreement with the upregulation of JNK, c-Jun phosphorylation at the JNK phosphorylation site of Ser 63 was increased in the skeletal muscles of regenerating *Mkp-5*$^{-/-}$ mice (Supplemental Figures 5 and 6). The expression of p53 increased in response to injury (Supplemental Figure 7, A and B), and this was also elevated in regenerating skeletal muscle derived from *Mkp5*$^{-/-}$ mice compared with that from *Mkp5*$^{+/+}$ mice (Supplemental Figure 7, C and D). Notably, other major pathways involved in regenerative myogenesis, such as Akt and S6 kinase 1, were found to be unchanged (Supplemental Figures 5 and 6). Therefore, MKP-5 exerts selective regulation on the cell cycle during skeletal muscle regeneration.

We next followed up on our observation that MKP-5 appears to negatively regulate cyclin D3 expression during regenerative myogenesis. To more directly examine the expression levels of the cyclins in the population of proliferating SCs, we isolated skeletal muscle cells that had regenerated for 2 days from *Mkp5*$^{+/+}$ and *Mkp5*$^{-/-}$ mice. Consistent with the results obtained from skeletal muscle, we found that PAX7$^+$ cells (Figure 7A) from *Mkp5*$^{-/-}$ mice expressed significantly increased levels of cyclin D3, but not cyclin D1 or D2, compared with *Mkp5*$^{+/+}$ mice (Figure 7, B–D). The expression levels of both CDK4 and CDK6 also remained unchanged (Figure 7, E and F). These results identify cyclin D3 as a downstream target of MKP-5 and suggest that MKP-5 suppresses SC proliferation by negatively regulating cyclin D3.

MKP-5 regulates SC proliferation through a JNK/cyclin D3–dependent pathway. To determine whether the effects of MKP-5 on MAPK signaling and cyclin D3 expression were SC autonomous, we measured MAPK activity and cyclin D3 levels in SC-derived myoblasts. We found that *Mkp5*$^{-/-}$ SC–derived myoblasts exhibited enhanced JNK and p38 MAPK, but not ERK1/2, phosphorylation in response to serum and increased cyclin D3 levels (Figure 8A). To identify which of the MAPKs conveys MKP-5 effects on SC proliferation, we performed clonal proliferation assays using MAPK inhibitors. We found that inhibition of JNK, but not p38 MAPK, rescued the hyperproliferation of *Mkp5*$^{-/-}$ SC–derived myoblasts (Figure 8B). Similar approaches using pharmacological inhibitors of the MAPK pathway were used to demonstrate that JNK was responsible for the increased expression of cyclin D3 in SC-derived myoblasts (Figure 8C). Collectively, these results indicate that MKP-5 regulates SC proliferation through a JNK/cyclin D3–dependent pathway.

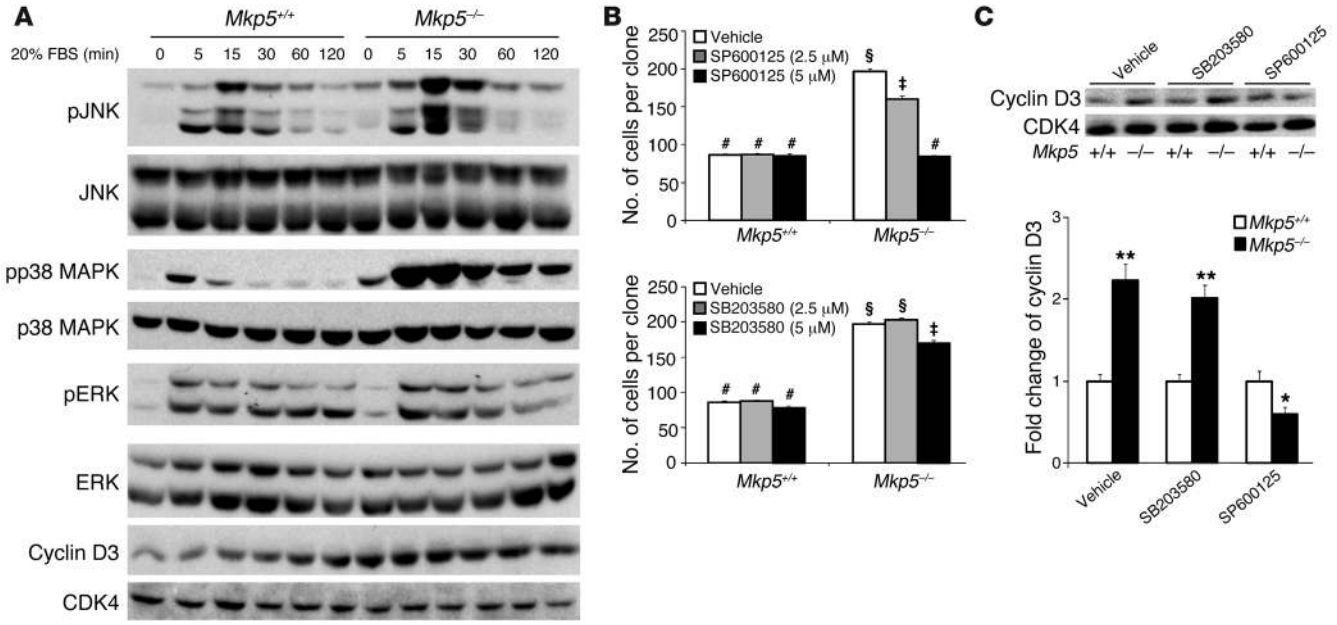

Figure 8

MKP-5 attenuates myoblast proliferation through a JNK/cyclin D3 pathway. (**A**) SC-derived myoblasts isolated from pooled hind limb muscles were serum starved overnight and then restimulated with 20% FBS for the indicated times. Immunoblots show phosphorylation of MAPKs and expression of cyclin D3. CDK4 serves as a loading control. (**B**) Clonal proliferation assays were performed in which SC-derived myoblasts were treated with either JNK (SP600125) or p38 MAPK (SB203580) inhibitors for 6 days. (**C**) Cyclin D3 expression in response to either JNK or p38 MAPK inhibitors (5 μM). (**A**–**C**) Results represent at least 3 independent preparations from 8-week-old male mice. For each independent preparation, 2 mice from each genotype were used. Results represent the mean ± SEM. *$P < 0.05$ and **$P < 0.01$ compared with *Mkp5*$^{+/+}$ mice. Symbols that differ (#, §, or ‡) indicate statistical significance between groups at $P < 0.05$.

To evaluate whether the increased cyclin D3 expression levels were responsible for the enhanced SC proliferation, and subsequently if this was dependent upon MKP-5, the expression levels of MKP-5 (Figure 9A) and cyclin D3 in C2C12 myoblasts (Figure 9B) were reduced by siRNA knockdown, either alone or in combination, and their proliferation was assessed. Both p38 MAPK and JNK, but not ERK1/2, were enhanced in differentiating myoblasts in which MKP-5 had been knocked down by siRNA treatment (Supplemental Figure 8). Knockdown of MKP-5 increased myoblast proliferation, whereas knockdown of cyclin D3 reduced it (Figure 9, C and E). However, when both MKP-5 and cyclin D3 were knocked down, the increased proliferation induced by the loss of MKP-5 was blocked (Figure 9, C and E). These results imply that MKP-5 suppresses myoblast proliferation by impairing JNK-mediated expression of cyclin D3. Because cyclin D3 is also a regulator of muscle cell differentiation (51, 53), we determined whether cyclin D3 knockdown impairs the enhanced differentiation incurred by loss of MKP-5. Knockdown of MKP-5 enhanced myoblast differentiation, as measured through the assessment of the myoblast fusion index (Figure 9, D and F). In contrast, cyclin D3 knockdown alone blocked myoblast fusion (Figure 9, D and F). When both MKP-5 and cyclin D3 levels were knocked down, the impairment in differentiation induced upon loss of cyclin D3 was restored in the background of cells lacking MKP-5 (Figure 9, D and F). These results demonstrate that although cyclin D3 plays a significant role in promoting myoblast differentiation, the suppressive effects of MKP-5 on myoblast differentiation likely occurs through either a p38 MAPK- and/or JNK-dependent pathway that is cyclin D3 independent.

Discussion

In this report, we have identified MKP-5 as an essential negative regulator of the promyogenic actions of MAPKs in mice. Based on these findings, we propose that MKP-5 maintains JNK and p38 MAPK in a dephosphorylated state, thereby maintaining SC quiescence (Figure 10). An important finding uncovered in this study is the demonstration that loss of MKP-5 in the *mdx* background is sufficient to markedly ameliorate the progression of muscular dystrophy. These results provide genetic evidence for a role of MKP-5 and the MAPK pathway in the progression of DMD and potentially other degenerative muscle diseases.

MKP-5–deficient mice exhibited enhanced MAPK activity in skeletal muscle and in SCs, with a rank order of dephosphorylation toward p38 MAPK and JNK, but not ERK1/2. MKP-5 is highly enriched in skeletal muscle (46, 47), suggesting that it plays an important role in this tissue. This notion was supported by the observation that skeletal muscle mass was greater in *Mkp5*$^{-/-}$ mice compared with that in wild-type mice, although this did not result in significant differences in the baseline strength properties of *Mkp5*$^{-/-}$mice. The increase in skeletal muscle mass is likely a reflection of increased myofiber size in *Mkp5*$^{-/-}$ mice. These results are consistent with other observations that the MAPKs are involved in determining skeletal muscle mass (40).

MKP-5 expression becomes downregulated in response to skeletal muscle damage, and JNK is hyperactivated in *Mkp5*$^{-/-}$ muscles, suggesting that MKP-5 downregulation facilitates the activation of JNK in order to trigger SC proliferation. Later on during regenerative myogenesis, p38 MAPK was hyperactivated in the skeletal

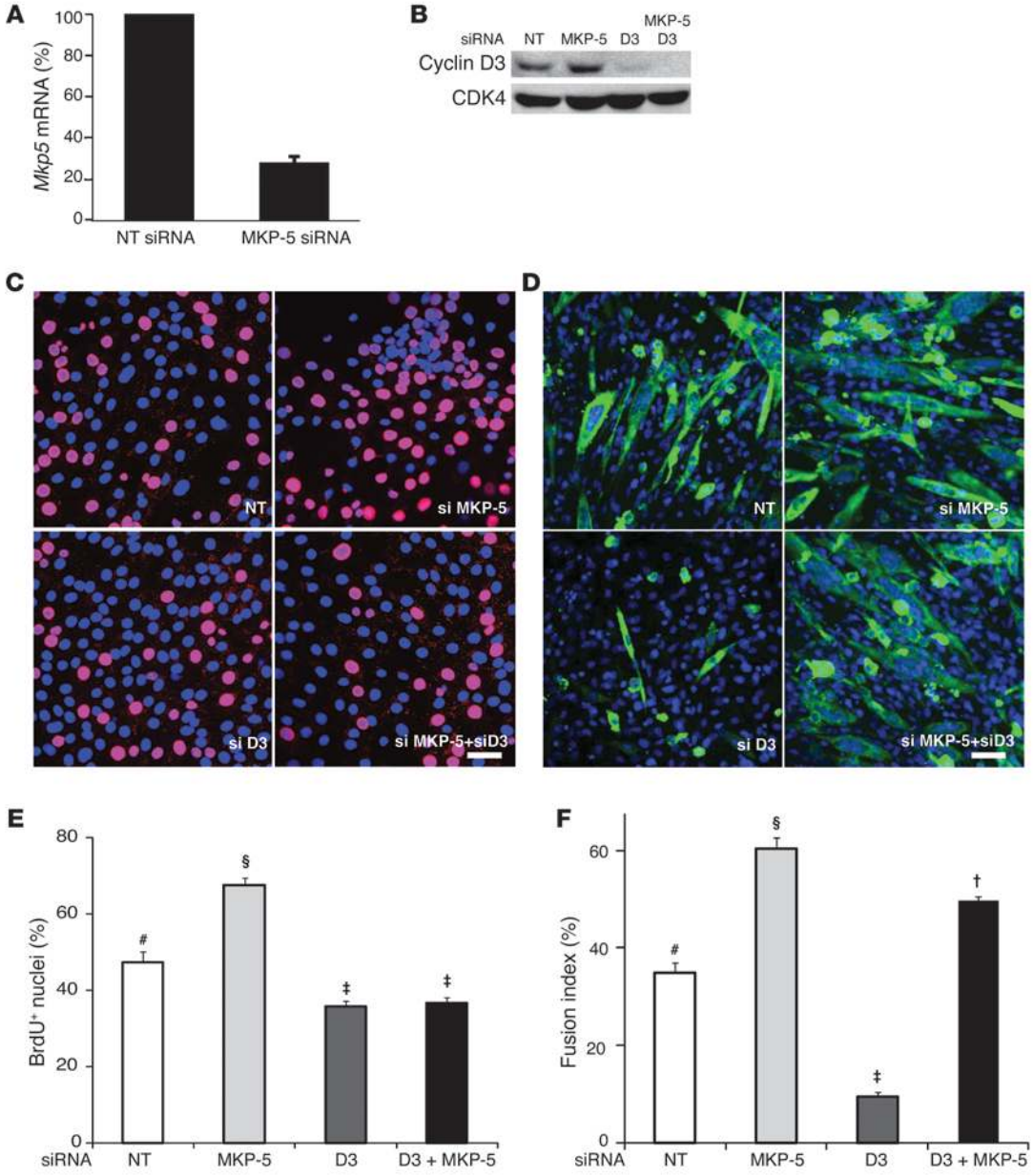

Figure 9

Effect of MKP-5 and cyclin D3 on myoblast proliferation and differentiation. (**A**) C2C12 myoblasts were transfected with MKP-5 siRNA. Twenty-four hours later, cell lysates were analyzed for *Mkp5* mRNA expression by quantitative PCR. (**B**) C2C12 cells were knocked down with cyclin D3 and/or MKP-5 siRNA. Forty-eight hours later, cell lysates were immunoblotted with cyclin D3 and CDK4 antibodies. (**C**) Effect of MKP-5 and/or cyclin D3 knockdown on myoblast proliferation. Seventy-two hours after siRNA transfection, myoblasts were pulsed with BrdU (10 μM) for 3 hours. Immunofluorescence images of C2C12 cells stained with TO-PRO-3 (blue, nuclei) and BrdU (red). Merged images show $BrdU^+$ cells in pink. Scale bar: 50 μm. (**D**) Myoblasts with MKP-5 or cyclin D3 knockdown were plated at equal numbers and transferred to DM for 60 hours. Scale bar: 50 μm. (**E**) Cells were treated as in **C**. Data show quantification of the percentage of $BrdU^+$ nuclei to total nuclei. (**F**) Cells were treated as in **D**. Fusion index was calculated as the percentage of nuclei (blue) within myosin heavy chain–positive myotubes (≥2 nuclei) divided by the total number of nuclei. (**A**–**F**) Results represent the mean ± SEM from at least 3 independent preparations. Symbols that differ (#, §, ‡, or †) indicate statistical significance between groups at $P < 0.05$. NT, nontargeted.

muscles of *Mkp5*$^{-/-}$ mice, consistent with the established role of p38 MAPK in promoting differentiation. The apparent effectiveness of MKP-5 to serve as an essential MKP for p38 MAPK and JNK during regeneration is also likely to be related to the expression status of other MKPs in skeletal muscle. For example, it has been shown that MKP-1 becomes transiently activated at the early stages of skeletal muscle regeneration (54). The induction of MKP-1, and possibly other MKPs, at this time point might account for the comparable levels of p38 MAPK phosphorylation at 2 days after injury in *Mkp5*$^{-/-}$ mice compared with wild-type mice. These

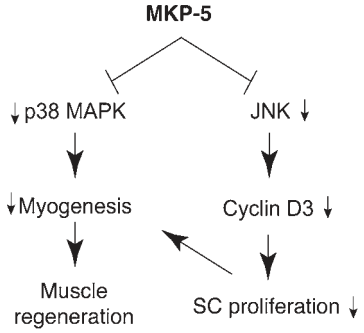

Figure 10
Model for the mechanism of MKP-5 in SC function and regenerative myogenesis.

results demonstrate that in response to skeletal muscle injury, MKP-5 temporally regulates the activities of both JNK and p38 MAPK in order to maintain the appropriate homeostatic control of these MAPKs, which coordinate regenerative myogenesis.

We show that loss of MKP-5 results in enhanced p38 MAPK and JNK activation, though only the inhibition of JNK appeared capable of promoting SC quiescence by the suppression of cyclin D3. The role of JNK in SC function has remained less clear in contrast to that of p38 MAPK. However, JNK activity has been shown to be required for both myoblast proliferation and differentiation (21, 32, 55). The results presented here support the interpretation that JNK is required for SC proliferation. The ability of MKP-5 to inactivate p38 MAPK is also consistent with the promyogenic role of p38 MAPK in both SC proliferation and differentiation (21, 24). SC-derived myoblasts from *Mkp5*$^{-/-}$ mice or MKP-5 siRNA–treated SC-derived myoblasts from wild-type mice exhibited increased differentiation. Therefore, these findings are supportive of the interpretation that MKP-5 plays an essential role in negatively regulating the physiologically relevant pool of JNK and p38 MAPK in the control of SC function and regenerative myogenesis (Figure 10).

The immune response plays a major role in the efficacy of the repair process. Given that *Mkp5*$^{-/-}$ mice exhibited improved muscle repair, it was important to assess the extent of the inflammatory response in damaged skeletal muscles from *Mkp5*$^{-/-}$ mice. We observed equivalent levels of both macrophage and neutrophil infiltrates in the damaged areas of skeletal muscle from *Mkp5*$^{+/+}$ and *Mkp5*$^{-/-}$ mice. This result was somewhat surprising, given previous findings of a negative regulatory role of MKP-5 in innate and adaptive immunity (44, 45). We cannot exclude the possibility that the repertoire of macrophage subpopulations is altered in a manner that promotes repair. Nonetheless, the inflammatory response in the context assessed here does not appear to play a deleterious role in the enhanced regenerative response in *Mkp5*$^{-/-}$ mice.

One of the most striking observations from this study is that the loss of MKP-5 is sufficient to markedly ameliorate the dystrophic phenotype of *mdx* mice. Although *mdx* mice succumb to a very mild dystrophic phenotype compared with humans, we were still able to observe an improvement in the dystrophic phenotype in *mdx* mice lacking MKP-5. Remarkably, *mdx* mice lacking MKP-5 expression demonstrated parameters of muscle function that were equivalent to those of wild-type C57BL/10 mice. Importantly, we demonstrated that in *mdx* mice lacking MKP-5, both p38 MAPK and JNK phosphorylation were enhanced compared with *mdx* mice. These results demonstrate that even in the absence of dystrophin, augmenting the activity of the MAPKs through specific loss of MKP-5 can ameliorate the progressive degeneration of skeletal muscle function in *mdx* mice. Mice lacking MKP-5 exhibit comparable levels of muscle strength compared with wild-type mice. Hence, the maintenance of muscle function in MKP-5–deficient *mdx* mice stems from the postdevelopmental effects of MKP-5 on the progression of the disease rather than from those conferred during development. Along these lines, SC-derived myoblasts from adult wild-type mice also exhibit increased proliferation and differentiation when MKP-5 expression is acutely reduced by siRNA. Hence, the actions of MKP-5 on MAPK signaling in SCs and regenerative myogenesis target processes that postdevelopmentally operate downstream of, and/or parallel to, dystrophin.

To support the supposition that MKP-5 was acting autonomously in SCs, we demonstrated that SCs derived from *Mkp5*$^{-/-}$ mice exhibited an enhanced proliferative response following injury. Several lines of evidence support this. First, following injury, *Mkp5*$^{-/-}$ SCs were found to expand nearly 3 times more rapidly than SCs from skeletal muscles of *Mkp5*$^{+/+}$ mice. Second, in vivo proliferation assays demonstrated that *Mkp5*$^{-/-}$ SCs proliferated more rapidly than *Mkp5*$^{+/+}$ SCs. Third, both clonal and single myofiber assays showed that *Mkp5*$^{-/-}$ SC–derived myoblasts exhibited increased proliferation compared with *Mkp5*$^{+/+}$ SC–derived myoblasts. Finally, acute depletion of MKP-5 by siRNA in SC-derived myoblasts from wild-type mice also enhanced cell proliferation, ruling out the possibility that MKP-5 loss during development was responsible for this effect. Since SC proliferation represents a major factor in the process of regenerative myogenesis, it is reasonable to surmise that the enhanced repair of skeletal muscle in both the acute and chronic paradigms of muscle injury stems from the increased levels of SC proliferation in mice lacking MKP-5.

We discovered that the expression of cyclin D3, but not cyclin D1 or cyclin D2, was enhanced in regenerating skeletal muscle from *Mkp5*$^{-/-}$ mice. Isolation of MKP-5–deficient SC-derived myoblasts confirmed that cyclin D3 was indeed upregulated in SCs, along with a concomitant upregulation of both p38 MAPK and JNK, but not ERK1/2. Thus, MKP-5 plays an essential role in negatively regulating SC proliferation through JNK-dependent regulation of cyclin D3. Cyclin D3 is induced during terminal differentiation, regulates myoblast cell-cycle exit, and is required for myogenic differentiation (51–53, 56, 57). In order to substantiate the relationship between MKP-5 and cyclin D3 in myoblast proliferation, we asked whether loss of cyclin D3 could rescue the enhanced proliferation in MKP-5–deficient muscle cells. These experiments revealed that elimination of cyclin D3 expression in the background of MKP-5 loss rescues the enhanced proliferative effects in MKP-5–deficient muscle cells. Hence, cyclin D3 is a major downstream target of MKP-5/JNK in the control of SC proliferation. Myoblasts deficient in p38 MAPK have been shown to reduce cyclin D3 levels, and loss of cyclin D3 inhibits myogenic gene activation (51, 56). In addition, cyclin D3 is transcriptionally activated through the AP-1/c-Jun module. Our data are consistent with MKP-5 regulation of SC proliferation through JNK/c-Jun/cyclin D3, rather than through p38 MAPK. Despite the fact that cyclin D3 is required for differentiation, MKP-5–mediated suppression of the differentiation pathway appeared to occur even when cyclin D3 expression was eliminated. These results suggest that MKP-5 suppresses differentiation through pathways other than those mediated by cyclin D3, but is dependent on JNK and/or p38 MAPK.

We have shown previously that MKP-1–deficient mice are impaired in their ability to undergo regenerative myogenesis and that SCs derived from these mice proliferate at a significantly slower rate (43). Moreover, when MKP-1–deficient mice are intercrossed with *mdx* mice, the dystrophic phenotype is exacerbated (43). These results suggest that despite the fact that MKP-1 also dephosphorylates JNK and p38 MAPK, it is unlikely to represent the physiologically relevant MKP that dephosphorylates the pool of MAPKs involved in maintaining SC quiescence. The mechanistic basis for why MKP-5, but not MKP-1, antagonizes SC proliferation remains unclear, although there are several possible explanations. One explanation is that MKP-5 is expressed in both the nucleus and cytosol (58), whereas MKP-1 is expressed exclusively in the nucleus (59). These differences in localization may result in the regulation of functionally distinct pools of MAPKs between MKP-5 and MKP-1, and hence the regulation of downstream MAPK substrates. In addition, MKP-1 expression is regulated in a distinct manner during regenerative myogenesis (54) compared with MKP-5. Finally, MKP-1–deficient mice exhibit a profound immunological phenotype following muscle damage (43), whereas MKP-5–deficient mice do not show such effects compared with wild-type mice. Together, these differences could explain the distinct phenotypes in SCs and regenerative myogenesis in MKP-1– and MKP-5–deficient mice. Interestingly, nonoverlapping functionalities between MKP-1 and MKP-5 in vascular injury have been reported previously (45). These observations highlight the complexities of physiological and pathophysiological MKP/MAPK–mediated signaling in vivo. Nonetheless, the results reported here demonstrate that MKP-5 controls the pool of MAPKs that are required collectively to regulate downstream phosphorylation of targets involved in the maintenance of SC quiescence and attenuation of regenerative myogenesis.

In DMD, the SC pool is depleted as a result of futile rounds of degeneration and regeneration. The severity of the DMD phenotype has been linked to a loss of SC function. We suggest that the enhanced proliferation of MKP-5–deficient SCs is sufficient to counter the depletion of SCs in both the acute regenerative response and in *mdx* mice, thereby ameliorating the severity of the disease. Consistent with this notion, *mdx* mice lacking the RNA component of telomerase display impaired SC proliferation and a more severe phenotype resembling human DMD (17). The conclusions derived here do not exclude other important factors that contribute to DMD, such as the loss of skeletal muscle structural integrity. Presumably, the collective repertoire of MKP-5/MAPK targets will need to be identified in order to fully define how MKP-5 functions in the maintenance of SC homeostasis.

In summary, these data identify MKP-5 as an essential negative regulator of SC proliferation and differentiation. The identification of MKP-5 as an essential negative regulator of SC function and DMD pathogenesis raises the possibility that pharmacological targeting of MKP-5 may represent a novel strategy for the treatment of DMD and possibly other skeletal muscle degenerative diseases.

Methods

Reagents and antibodies. SB203580 and SP600125 were purchased from EMD Biosciences. CTX and Evans blue dye were obtained from Sigma-Aldrich. Anti-pERK1/2, pJNK, p38 MAPK, cyclin D3, and CDK4 antibodies were obtained from Cell Signaling Technology. ERK1/2, JNK, p38 MAPK, and MYF5 antibodies were purchased from Santa Cruz Biotechnology. 5′-bromo 2′-deoxyuridine (BrdU) and myosin heavy chain (MF20) antibodies were from Developmental Studies Hybridoma Bank. TO-PRO-3 iodide for nuclear staining was purchased from Invitrogen. See also Supplemental Methods for additional details on the antibodies.

Animal experiments. MKP-5 knockout mice were generated as described previously (44). To generate *mdx/Mkp5*$^{-/-}$ mice, male *Mkp5*$^{-/-}$ mice were crossed with female *mdx* mice, the F1 males were backcrossed with female *mdx* mice, and the resultant F2 offspring were then intercrossed.

Muscle damage analysis. Mice were anesthetized by administration of 10 mg/kg ketamine and 1 mg/kg xylazine. Muscle damage was induced by intramuscular injection of 50 μl CTX (Sigma-Aldrich, 0.1 mg/ml in PBS) into the tibialis anterior (TA) muscle longitudinally or 300 μl into the gastrocnemius/soleus muscles. At the indicated times (see Figure 2C), the damaged muscle was dissected and fixed in 10% neutral-buffered formalin overnight, washed twice in 70% ethanol, and paraffin embedded for H&E staining. For *mdx* muscle myopathy analyses, the degenerating area was counted as a combined total, with each area containing greater than or equal to 10 degenerating fibers, and the percentage of degenerating area was calculated as a percentage of the whole gastrocnemius muscle area. To evaluate *mdx* muscle fiber integrity, 1% Evans blue dye dissolved in sterile saline was administered by intraperitoneal injection at a dose of 1% of body weight. Twenty-four hours later, muscles were dissected and snap-frozen in isopentene precooled in liquid nitrogen. Muscle cryosections of 10-μm thickness were cut and Evans blue dye intake was evaluated using a Zeiss laser scanning confocal microscope (Carl Zeiss).

Muscle strength test. Grip tests were performed as previously described (43). To assess mouse forelimb strength, we used a Grip Strength Meter (Columbus Instruments) and allowed the mice to grip the horizontal bar attached to the front of the meter. Mice were pulled horizontally by the tail until the bar was released. Repetitions of this procedure were performed and the peak force was recorded for each mouse. To measure muscle-specific force and contraction-induced fatigue and recovery, the distal end of the EDL muscle was dissected and linked to a transducer (Kent Scientific). EDL muscle was stimulated with an S48 square pulse stimulator (Grass Technologies) and the output signals were captured and analyzed using a PowerLab data acquisition system with LabChart Pro software (ADInstruments).

Immunohistochemical and immunocytochemical staining. Muscles were fixed in 10% neutral-buffered formalin overnight, washed in 70% ethanol, and paraffin embedded. Muscles were cut into 10-μm-thick cross sections. Before staining, muscle sections were de-paraffinized with 2 changes of xylene for 5 minutes each time, rehydrated in 2 changes of 100% ethanol for 3 minutes each, and followed by 95% and 80% ethanol for 1 minute each time before rinsing in distilled H_2O. The sections were then immersed in sodium citrate buffer preheated to approximately 100°C in a steamer and incubated for 30 minutes. After the steaming process, the sections were allowed to cool at room temperature in the same buffer for 20 minutes before rinsing 3 times in PBS for 5 minutes each time. The sections were blocked in 5% goat serum for 60 minutes at room temperature before application of the primary and secondary antibodies. For nuclear staining, TO-PRO-3 was applied to the reaction together with the secondary antibody.

Myosin heavy chain immunocytochemical staining was conducted as described previously (43). For BrdU staining, cells were fixed in ice-cold 70% ethanol for 5 minutes followed by incubation in 1.5 M HCl for 30 minutes at room temperature. Cells were rinsed and stained with antibodies against BrdU. PAX7 immunohistochemical staining was carried out as described in Supplemental Methods.

SC functional analyses. SC-derived myoblasts were isolated and cultured as previously described (43). For proliferation assays, fiber-derived or FACS-sorted SCs (based on surface marker expression; CD34$^+$CD45$^-$Sca-1$^-$) (10) were grown in F-10 medium containing 20% FBS, and the number of cells per clone was calculated at the indicated time. For in vivo BrdU incorpo-

ration assays, BrdU (100 mg/kg) was injected intraperitoneally 24 hours after the TA muscles were damaged. Muscles were collected 18 hours later to stain for both BrdU and MYF5. To induce SC differentiation, growth medium was withdrawn and cells were washed twice with PBS and cultured in differentiation medium (DMEM containing 4% horse serum). Differentiated SCs were immunocytochemically stained with the differentiation marker myosin heavy chain antibody (MF20). The fusion index was calculated as the percentage of nuclei within myotubes containing at least 2 nuclei as a ratio of total nuclei in the field. For MAPK phosphorylation experiments, SCs were serum starved in F-10 containing 0.1% FBS overnight before switching to F-10 containing 20% FBS for the indicated time (see Figure 8A). For knockdown of MKP-5, SC-derived myoblasts were isolated from C57BL/6 muscles, preplated to enrich for myoblasts, and transfected with ON-TARGETplus nontargeting pool (siNT) and ON-TARGETplus SMART pool MKP-5 siRNA (siMKP-5) (Thermo Scientific) using Lipofectamine 2000 (Life Technologies) according to the manufacturer's instructions.

C2C12 myoblast culture. C2C12 myoblasts were cultured in DMEM containing 10% FBS. For siRNA knockdown experiments, C2C12 myoblasts were transfected with ON-TARGETplus SMART pool cyclin D3 or MKP-5 siRNA (Thermo Scientific) using DharmaFECT 1 reagent (Thermo Scientific). For BrdU incorporation, transfected cells were pulse-chased 72 hours later with 10 μM BrdU for 3 hours. For differentiation assays, myoblasts were shifted to differentiation medium (DMEM containing 0.1% FBS, 5 μg/ml insulin, 5 μg/ml selenium) for the indicated times (see Figure 9, D and F). The fusion index was calculated as the percentage of nuclei within myotubes containing at least 2 nuclei as a ratio of total nuclei in the field.

Flow cytometry. To sort for SCs, hind limb muscles were minced and digested with collagenase B/dispase II, filtered through 45-μm nylon cell strainers, and pelleted at 350 *g*. PE-CD45 and FITC-Sca-1 antibodies were purchased from BD Biosciences; biotin-CD34 and APC-streptavidin were from eBioscience. For FACS analysis of macrophage and neutrophil infiltration, muscles were damaged by CTX injection. Forty-two hours later, damaged muscles were isolated and digested with collagenase B/dispase II. The isolated cells were then stained with CD11b (Developmental Studies Hybridoma Bank) and 7/4 (AbD Serotec) antibodies, respectively. After a brief wash, FITC-conjugated secondary antibodies were applied and the cells were analyzed using a BD FACSCalibur flow cytometer (BD Biosciences). For FACS analysis of cell-cycle regulator protein levels, muscles were CTX-damaged for 2 days and then digested, and cells were isolated for staining. Rabbit anti-PAX7 antibody and mouse anti-cyclin D1, cyclin D2, and CDK4 were purchased from Abcam. Mouse anti–cyclin D3 was purchased from Thermo Scientific. Goat anti-CDK6 antibody was purchased from Santa Cruz Biotechnology. Secondary APC-conjugated anti-rabbit and FITC-conjugated anti-mouse or anti-goat antibody were obtained from Jackson ImmunoResearch.

Biochemical analysis. For immunoblotting, proteins were separated by 10% SDS-PAGE and transferred to PVDF membrane. The membrane was blocked in 7% nonfat dried milk for 1 hour at room temperature. After a brief wash in TBST, the membrane was incubated with primary antibody in 5% BSA overnight at 4°C. After three 5-minute washes in TBST, the membrane was incubated with an HRP-conjugated secondary antibody for 1 hour at room temperature. The membrane was developed using ECL reagents (GE Healthcare). See Supplemental Methods for additional details.

Kinase activity assays. MAPK activity assays were performed as described previously (42). Serum creatine kinase was assayed using the EnzyChrom Creatine Kinase Assay kit (BioAssay Systems) according to the manufacturer's instructions.

Quantitative RT-PCR. Total RNA from cells or skeletal muscles was extracted using TRIzol reagent (Life Technologies), and genomic DNA was removed using a DNA-free kit (Applied Biosystems). cDNA was synthesized using a High Capacity cDNA Reverse Transcription kit (Applied Biosystems). For quantitative PCR, TaqMan MKP-5 and 18S rRNA primers were used in combination with the TaqMan Gene Expression Master Mix (Applied Biosystems) in a total reaction of 20 μl. A 7500 Fast-Real Time PCR System (Applied Biosystems) was used to quantify mRNA expression. *Mkp5* mRNA relative abundance was normalized to internal control 18S rRNA and expressed as percentage change in either the nondamaged muscle or nontargeted siRNA where indicated in Figures 2A and 9A.

Statistics. Statistical analysis was performed using the Student's *t* test with 2-tailed distribution, assuming normal distribution and equal variance among different samples. Data are presented as the means ± SEM. Statistical significance is signified as $*P < 0.05$, $**P < 0.01$, and $***P < 0.001$. Where appropriate, symbols were used for comparison; data points with symbols that differ signify a statistical significance of $P < 0.05$, with the same symbol signifying no statistical significance between samples.

Study approval. The Yale University Institutional Animal Care and Use Committee approved all procedures.

Acknowledgments

We thank Dake Qi and Lawrence H. Young (Yale School of Medicine) for assistance with the muscle contraction experiments. We also thank Gerald I. Shulman (Department of Endocrinology/Internal Medicine, Yale School of Medicine) for Minispec analysis of muscle mass. This work was supported by NIH grants (AR46504 and DK075776, to A.M. Bennett) and a Muscular Dystrophy Association grant (MDA 186936, to H. Shi).

Received for publication April 17, 2012, and accepted in revised form January 31, 2013.

Address correspondence to: Anton M. Bennett, Yale University School of Medicine, Department of Pharmacology, SHM B226D, 333 Cedar Street, New Haven, Connecticut 06520-8066, USA. Phone: 203.737.2441; Fax: 203.737.2738; E-mail: anton.bennett@yale.edu.

1. Hawke TJ, Garry DJ. Myogenic satellite cells: physiology to molecular biology. *J Appl Physiol*. 2001;91(2):534–551.
2. Seale P, Rudnicki MA. A new look at the origin, function, and "stem-cell" status of muscle satellite cells. *Dev Biol*. 2000;218(2):115–124.
3. Wagers AJ, Conboy IM. Cellular and molecular signatures of muscle regeneration: current concepts and controversies in adult myogenesis. *Cell*. 2005;122(5):659–667.
4. Shi X, Garry DJ. Muscle stem cells in development, regeneration, and disease. *Genes Dev*. 2006; 20(13):1692–1708.
5. Buckingham M, Montarras D. Skeletal muscle stem cells. *Curr Opin Genet Dev*. 2008;18(4):330–336.
6. Kuang S, Kuroda K, Le Grand F, Rudnicki MA. Asymmetric self-renewal and commitment of satellite stem cells in muscle. *Cell*. 2007;129(5):999–1010.
7. Bischoff R. Chemotaxis of skeletal muscle satellite cells. *Dev Dyn*. 1997;208(4):505–517.
8. Rudnicki MA, Le Grand F, McKinnell I, Kuang S. The molecular regulation of muscle stem cell function. *Cold Spring Harb Symp Quant Biol*. 2008; 73:323–331.
9. Tedesco FS, Dellavalle A, Diaz-Manera J, Messina G, Cossu G. Repairing skeletal muscle: regenerative potential of skeletal muscle stem cells. *J Clin Invest*. 2010;120(1):11–19.
10. Montarras D, et al. Direct isolation of satellite cells for skeletal muscle regeneration. *Science*. 2005; 309(5743):2064–2067.
11. Nishino I, Ozawa E. Muscular dystrophies. *Curr Opin Neurol*. 2002;15(5):539–544.
12. Porter JD. Introduction to muscular dystrophy. *Microsc Res Tech*. 2000;48(3–4):127–130.
13. Hoffman EP, Brown RH Jr, Kunkel LM. Dystrophin: the protein product of the Duchenne muscular dystrophy locus. *Cell*. 1987;51(6):919–928.
14. Petrof BJ, Shrager JB, Stedman HH, Kelly AM, Sweeney HL. Dystrophin protects the sarcolemma from stresses developed during muscle contraction. *Proc Natl Acad Sci U S A*. 1993;90(8):3710–3714.

15. Bhatnagar S, Kumar A. Therapeutic targeting of signaling pathways in muscular dystrophy. *J Mol Med (Berl)*. 2010;88(2):155–166.
16. Blau HM, Webster C, Pavlath GK. Defective myoblasts identified in Duchenne muscular dystrophy. *Proc Natl Acad Sci U S A*. 1983;80(15):4856–4860.
17. Sacco A, et al. Short telomeres and stem cell exhaustion model Duchenne muscular dystrophy in mdx/mTR mice. *Cell*. 2010;143(7):1059–1071.
18. Cuenda A, Cohen P. Stress-activated protein kinase-2/p38 and a rapamycin-sensitive pathway are required for C2C12 myogenesis. *J Biol Chem*. 1999; 274(7):4341–4346.
19. Weston AD, Sampaio AV, Ridgeway AG, Underhill TM. Inhibition of p38 MAPK signaling promotes late stages of myogenesis. *J Cell Sci*. 2003; 116(pt 14):2885–2893.
20. Kondoh K, Sunadome K, Nishida E. Notch signaling suppresses p38 MAPK activity via induction of MKP-1 in myogenesis. *J Biol Chem*. 2007; 282(5):3058–3065.
21. Perdiguero E, et al. Genetic analysis of p38 MAP kinases in myogenesis: fundamental role of p38-alpha in abrogating myoblast proliferation. *EMBO J*. 2007;26(5):1245–1256.
22. Lluis F, Perdiguero E, Nebreda AR, Munoz-Canoves P. Regulation of skeletal muscle gene expression by p38 MAP kinases. *Trends Cell Biol*. 2006;16(1):36–44.
23. Keren A, Tamir Y, Bengal E. The p38 MAPK signaling pathway: a major regulator of skeletal muscle development. *Mol Cell Endocrinol*. 2006;252(1–2):224–230.
24. Jones NC, et al. The p38alpha/beta MAPK functions as a molecular switch to activate the quiescent satellite cell. *J Cell Biol*. 2005;169(1):105–116.
25. Gredinger E, Gerber AN, Tamir Y, Tapscott SJ, Bengal E. Mitogen-activated protein kinase pathway is involved in the differentiation of muscle cells. *J Biol Chem*. 1998;273(17):10436–10444.
26. Milasincic DJ, Calera MR, Farmer SR, Pilch PF. Stimulation of C2C12 myoblast growth by basic fibroblast growth factor and insulin-like growth factor 1 can occur via mitogen-activated protein kinase-dependent and -independent pathways. *Mol Cell Biol*. 1996;16(11):5964–5973.
27. Coolican SA, Samuel DS, Ewton DZ, McWade FJ, Florini JR. The mitogenic and myogenic actions of insulin-like growth factors utilize distinct signaling pathways. *J Biol Chem*. 1997;272(10):6653–6662.
28. Weyman CM, Ramocki MB, Taparowsky EJ, Wolfman A. Distinct signaling pathways regulate transformation and inhibition of skeletal muscle differentiation by oncogenic Ras. *Oncogene*. 1997; 14(6):697–704.
29. Jones NC, Fedorov YV, Rosenthal RS, Olwin BB. ERK1/2 is required for myoblast proliferation but is dispensable for muscle gene expression and cell fusion. *J Cell Physiol*. 2001;186(1):104–115.
30. Gallo R, Serafini M, Castellani L, Falcone G, Alem S. Distinct effects of Rac1 on differentiation of primary avian myoblasts. *Mol Biol Cell*. 1999; 10(10):3137–3150.
31. Meriane M, Charrasse S, Comunale F, Gauthier-Rouviere C. Transforming growth factor beta activates Rac1 and Cdc42Hs GTPases and the JNK pathway in skeletal muscle cells. *Biol Cell*. 2002;94(7–8):535–543.
32. Khurana A, Dey CS. Involvement of c-Jun N-terminal kinase activities in skeletal muscle differentiation. *J Muscle Res Cell Motil*. 2004;25(8):645–655.
33. Dickinson RJ, Keyse SM. Diverse physiological functions for dual-specificity MAP kinase phosphatases. *J Cell Sci*. 2006;119(pt 22):4607–4615.
34. Owens DM, Keyse SM. Differential regulation of MAP kinase signalling by dual-specificity protein phosphatases. *Oncogene*. 2007;26(22):3203–3213.
35. Boutros T, Chevet E, Metrakos P. Mitogen-activated protein (MAP) kinase/MAP kinase phosphatase regulation: roles in cell growth, death, and cancer. *Pharmacol Rev*. 2008;60(3):261–310.
36. Lawan A, Shi H, Gatzke F, Bennett AM. Diversity and specificity of the mitogen-activated protein kinase phosphatase-1 functions. *Cell Mol Life Sci*. 2013; 70(2):223–237.
37. Bennett AM, Tonks NK. Regulation of distinct stages of skeletal muscle differentiation by mitogen-activated protein kinases. *Science*. 1997; 278(5341):1288–1291.
38. Roth RJ, et al. MAPK phosphatase-1 facilitates the loss of oxidative myofibers associated with obesity in mice. *J Clin Invest*. 2009;119(12):3817–3829.
39. Shi H, et al. Modulation of skeletal muscle fiber type by mitogen-activated protein kinase signaling. *FASEB J*. 2008;22(8):2990–3000.
40. Shi H, et al. Mitogen-activated protein kinase signaling is necessary for the maintenance of skeletal muscle mass. *Am J Physiol Cell Physiol*. 2009; 296(5):C1040–C1048.
41. Shi H, Zeng C, Ricome A, Hannon KM, Grant AL, Gerrard DE. Extracellular signal-regulated kinase pathway is differentially involved in beta-agonist-induced hypertrophy in slow and fast muscles. *Am J Physiol Cell Physiol*. 2007;292(5):C1681–C1689.
42. Wu JJ, et al. Mice lacking MAP kinase phosphatase-1 have enhanced MAP kinase activity and resistance to diet-induced obesity. *Cell Metabolism*. 2006;4(1):61–73.
43. Shi H, et al. MAP kinase phosphatase-1 deficiency impairs skeletal muscle regeneration and exacerbates muscular dystrophy. *FASEB J*. 2010;24(8):2985–2997.
44. Zhang Y, et al. Regulation of innate and adaptive immune responses by MAP kinase phosphatase 5. *Nature*. 2004;430(7001):793–797.
45. Qian F, et al. A non-redundant role for MKP5 in limiting ROS production and preventing LPS-induced vascular injury. *EMBO J*. 2009;28(19):2896–2907.
46. Theodosiou A, Smith A, Gillieron C, Arkinstall S, Ashworth A. MKP5, a new member of the MAP kinase phosphatase family, which selectively dephosphorylates stress-activated kinases. *Oncogene*. 1999;18(50):6981–6988.
47. Masuda K, Shima H, Kikuchi K, Watanabe Y, Matsuda Y. Expression and comparative chromosomal mapping of MKP-5 genes DUSP10/Dusp10. *Cytogenet Cell Genet*. 2000;90(1–2):71–74.
48. Stedman HH, et al. The mdx mouse diaphragm reproduces the degenerative changes of Duchenne muscular dystrophy. *Nature*. 1991; 352(6335):536–539.
49. Suelves M, et al. uPA deficiency exacerbates muscular dystrophy in MDX mice. *J Cell Biol*. 2007; 178(6):1039–1051.
50. Shea KL, et al. Sprouty1 regulates reversible quiescence of a self-renewing adult muscle stem cell pool during regeneration. *Cell Stem Cell*. 2010; 6(2):117–129.
51. Cenciarelli C, et al. Critical role played by cyclin D3 in the MyoD-mediated arrest of cell cycle during myoblast differentiation. *Mol Cell Biol*. 1999; 19(7):5203–5217.
52. Kiess M, Gill RM, Hamel PA. Expression of the positive regulator of cell cycle progression, cyclin D3, is induced during differentiation of myoblasts into quiescent myotubes. *Oncogene*. 1995;10(1):159–166.
53. De Santa F, Albini S, Mezzaroma E, Baron L, Felsani A, Caruso M. pRb-dependent cyclin D3 protein stabilization is required for myogenic differentiation. *Mol Cell Biol*. 2007;27(20):7248–7265.
54. Szelenyi ER, Urso ML. Time-course analysis of injured skeletal muscle suggests a critical involvement of ERK1/2 signaling in the acute inflammatory response. *Muscle Nerve*. 2012;45(4):552–561.
55. Alter J, Rozentzweig D, Bengal E. Inhibition of myoblast differentiation by tumor necrosis factor alpha is mediated by c-Jun N-terminal kinase 1 and leukemia inhibitory factor. *J Biol Chem*. 2008; 283(34):23224–23234.
56. Wang H, Xu Q, Xiao F, Jiang Y, Wu Z. Involvement of the p38 mitogen-activated protein kinase alpha, beta, and gamma isoforms in myogenic differentiation. *Mol Biol Cell*. 2008;19(4):1519–1528.
57. Rao SS, Kohtz DS. Positive and negative regulation of D-type cyclin expression in skeletal myoblasts by basic fibroblast growth factor and transforming growth factor β. *J Biol Chem*. 1995;270(8):4093–4100.
58. Tanoue T, Moriguchi T, Nishida E. Molecular cloning and characterization of a novel dual specificity phosphatase, MKP-5. *J Biol Chem*. 1999; 274(28):19949–19956.
59. Wu JJ, Zhang L, Bennett AM. The noncatalytic amino terminus of mitogen-activated protein kinase phosphatase 1 directs nuclear targeting and serum response element transcriptional regulation. *Mol Cell Biol*. 2005;25(11):4792–4803.